Electronic Supplementary Material (ESI) for Inorganic Chemistry Frontiers.

Electronic Supplementary Information

Rough Endoplasmic Reticulum-like VSe_2/rGO Anode for Superior Sodium-Ion Capacitors

Yuanke Wu, Hao Chen, Longcheng Zhang, Qiulin Li, Maowen Xu* and Shu-juan Bao*

1 Institute for Clean Energy & Advanced Materials, School of Materials and Energy, Southwest University, Chongqing 400715, PR China

2 State Key Laboratory of Silkworm Genome Biology, Southwest University, Chongqing 400715, P. R. China

3 Chongqing Engineering and Technology Research Center for Novel Silk Materials, Southwest University, Chongqing 400715, P. R. China

*Corresponding author.E-mail: xumaowen@swu.edu.cn; baoshj@swu.edu.cn

1. Materials Characterization.

The X-ray diffraction (XRD, Shimadzu-7000) measurements were used to collect the crystal structure information of samples. Field emission scanning electron microscopy (FESEM, JSM-7800F) and transmission electron microscopy (TEM, JEOL2100, 200kV) were used to observe the morphologies and microstructure of as-prepared samples. X-ray photoelectron spectrosc-opy (XPS, Escalab 250xi) was used to investigate the surface composition and valence state information. The thermogravimetric analysis (TGA, Thermo Gravimetric Analyzer Q50) was used to estimate the carbon content of samples. The Brunauer-Emmett-Teller (BET) surface area was obtained using an Autosorb-1 (Quantachrome Instruments), and the pore size distribution was calculated according to the density functional theory (DFT) method.

2. Electrochemical Measurement

The CV curves were measured on CHI 760E electrochemical workstation (CHI Instruments Inc.). Galvanostatic charge/discharge measurements were carried out on a multi-channel battery testing system (LAND CT2001A). The voltage window for the half-cell was 0.01-3 V vs. Na/Na^+, while the voltage window for the full sodium ion hybrid devices was 1-4 V. Electrochemical impedance spectra (EIS) were performed on a Zahner Ennium electro-chemical workstation (Zennium, IM6, Germany) with the frequency range from 10^{-2} to 10^5 Hz. The energy and power densities of full-cells were calculated according to the following **Equation 1-3**;

$$C = I \times \Delta t / \Delta V \qquad (1)$$

$$E = (C \times \Delta V^2)/2 \qquad (2)$$

$$P = E/\Delta t \qquad (3)$$

Where C (F g^{-1}) is specific capacity; I (A g^{-1}) is the charge/discharge current, ΔV is the working voltage, Δt is discharge time (s), and E (Wh kg^{-1}) corresponds to the energy density and P (W kg^{-1}) is the power density.

3. Calculations of carbon content in 3D VSe_2/rGO aeroge

$$4VSe_2+13O_2=2V_2O_5+2SeO_2\uparrow$$

The carbon content in 3D VSe_2/rGO aerogel is calculated by **Equation 4;**

$$70.31\%m = 59.58\%mn + m(1-n) \qquad (4)$$

m represents the total mass of VSe_2/rGO aerogel, n is the percentage composition of VSe_2 in the VSe_2/rGO aerogel.

As shown in **Figure 2**h, the weight loss of VSe_2 and VSe_2/rGO aerogel are 59.58% and 74.58%, respectively. The weight percentage of both samples increased slightly between 200-400 ℃, which may be due to the formation of VO_2 and SeO_2. Significant mass loss occurred in both samples after 400℃ due to sublimation of SeO_2 and oxidation of C. The carbon content in VSe_2/rGO aerogel can be calculated from **Equation 4**. Consequently, the VSe_2 loading in VSe_2/ rGO aerogel calculated to be 73.46%.

4. The related reaction equations of VSe_2/rGO electrode druing charge and discharge.

Discharge process:

$$VSe_2 + x\mathrm{Na}^+ + xe^- Na_xVSe_2 \quad (5)$$

$$Na_xVSe_2 + (2-x)Na^+ + (2-x)e^- \rightarrow VSe + Na_2Se \quad (6)$$

$$VSe + 2\mathrm{Na}^+ + 2e^- \rightarrow V + Na_2Se \quad (7)$$

Charge process:

$$V + Na_2Se \rightarrow VSe + 2Na^+ + 2e^- \quad (8)$$

$$VSe + Na_2Se \rightarrow Na_xVSe_2 + (2-x)Na^+ + (2-x)e^- \quad (9)$$

$$Na_xVSe_2 \rightarrow VSe_2 + x\mathrm{Na}^+ + xe^- \quad (10)$$

5. The diffusion coefficient (D_{Na^+}) of sodium ions in host materials can be calculated from EIS according to the low frequency region from the following model and Equation 11 and Equation 12.

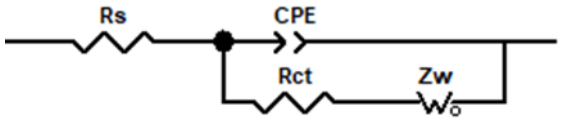

$$\mathrm{D} = \frac{R^2T^2}{2A^2n^4F^4C^2\sigma_\omega^2} \quad (11)$$

$$\mathrm{Z}' = R_s + R_{ct} + \sigma_\omega\omega^{-1/2} \quad (12)$$

In this model, Rs represents the bulk resistance of the cell; Rct corresponds to the charge transfer resistance; CPE depicts the double layer capacitance and passivation coating capacitance. Zw describes the Warburg impedance revealing the diffusion behavior of Na^+ at low frequency. In this equation, R, T, A, F, n, C and σ_ω represent the gas constant, absolute temperature, surface area of the work electrode, Faraday's constant, number of electrons per molecule during reaction, and Na^+ concentration in the in the electrolyte, Warburg factor

respectively.

Table 1. Kinetic parameters of 3D VSe_2/rGO aerogel, VSe_2 and 3D VO_2/rGO aerogel obtained from equivalent circuit fitting.

Anode material	Rct(Ω)	Diffusion coefficient ($cm^2\ s^{-1}$)
3D VSe_2/rGO aerogel	49.73	1.1383×10^{-13}
VSe_2	122.8	6.2727×10^{-15}
3D VO_2/rGO aerogel	107.5	1.3618×10^{-14}

Table 2. b value corresponding to each cathode peak and anode peak.

	b Value
peak 1	0.768687
peak 2	0.842444
peak 3	0.763649
peak 4	0.674008
peak 5	0.889216
peak 6	0.724054

6. **Calculate methods and details of capacitive effect contribution and diffusion-controlled contribution.**

$$i = av^b \qquad (13)$$

Where a and b are the adjustable parameters, b-value equal to 1 indicates charge storage is entirely from the capacitive-controlled process, while a b-value of 0.5 signifies a total diffusion-controlled reaction.

Using the scan-rate-dependent CV curves (**Figure 4**a) to quantify the contribution from capacitive effects (both surface pseudocapacitance and doublelayer capacitance) and diffusion-controlled Na^+ insertion process to the current response according to the following **Equation 14**;

$$I(V) = k_1 v + k_2 v^{1/2} \qquad (14)$$

Where $I(V)$, $k_1 v$ and $k_2 v^{1/2}$ represent the total current response at a given potential V, current due to surface capacitive effects, and current due to diffusion-controlled Na^+ insertion process, respectively. The above equation can also be reformulated as **Equation 15**;

$$I(V)/v^{1/2} = k_1 v^{1/2} + k_2 \qquad (15)$$

By plotting $I(V)/v^{1/2}$ vs. $v^{1/2}$ at different potentials, we can calculate the values of k_1 (slope) and k_2 (intercept) from the straight lines. After integration of the enclosed CV area, the amount of stored charge from different energy storage modes can be distinguished, expressed by the following **Equation 16**;

$$Q=Qs + Qd \quad (16)$$

Where, Q, Qs, and Qd represent the total stored charge included in the enclosed CV area at set scan rate, surface capacitive effects, and diffusion-controlled Na^+ insertion process, respectively.

Supplementary Figures

Fig. S1 Schematic illustration of the route for synthesis of 3D VSe_2/rGO aerogel.

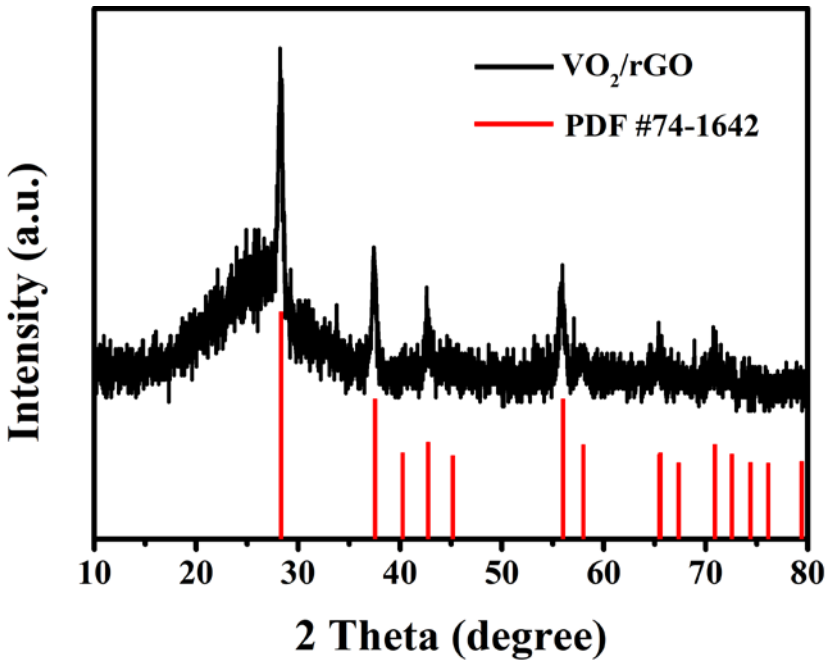

Fig. S2 XRD patterns VO_2/rGO.

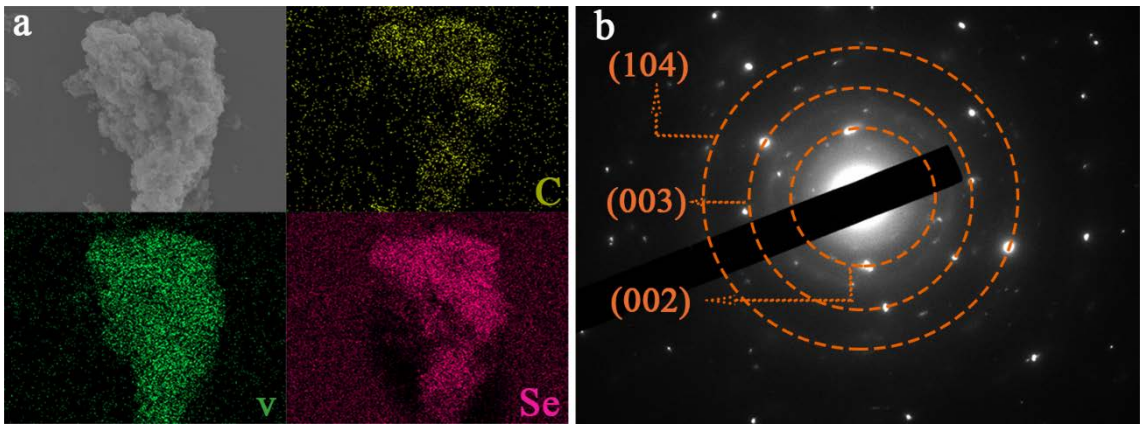

Fig. S3 (a) Element mapping images and (b) Selected electron diffraction area (SEDA) of VSe_2/rGO.

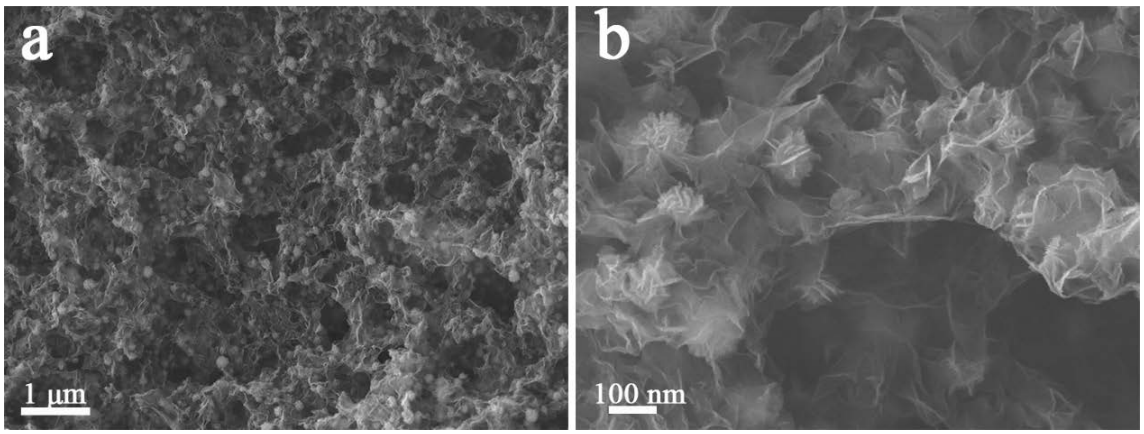

Fig. S4 FESEM images VO_2/rGO.

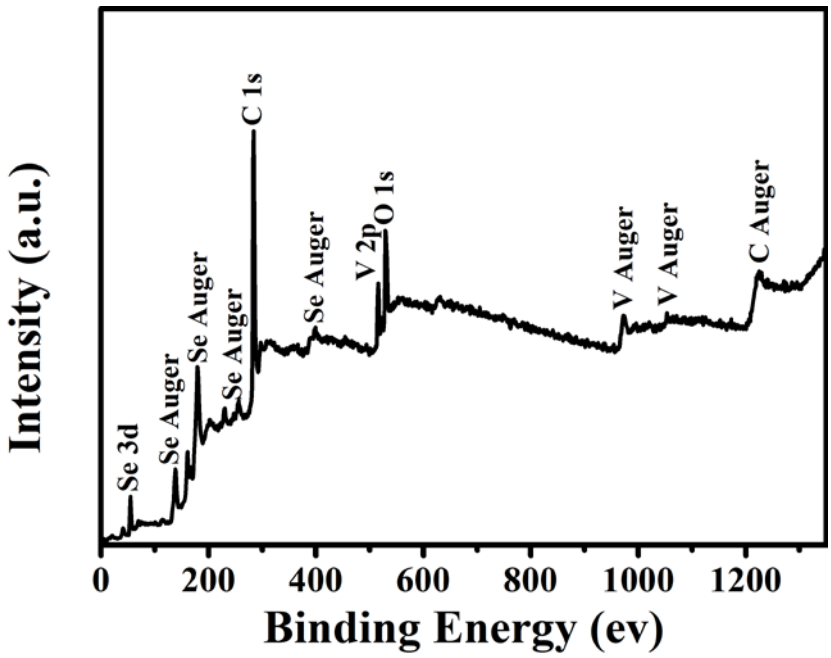

Fig. S5 XPS full spectra of VSe_2/rGO

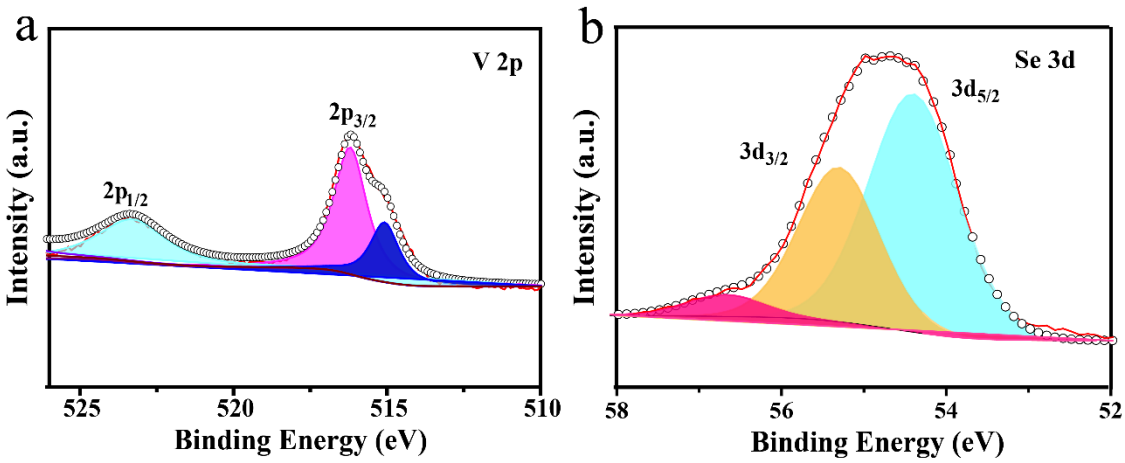

Fig. S6 (a) V 2p and (b) Se 3d XPS spectra of VSe_2/rGO, respectively.

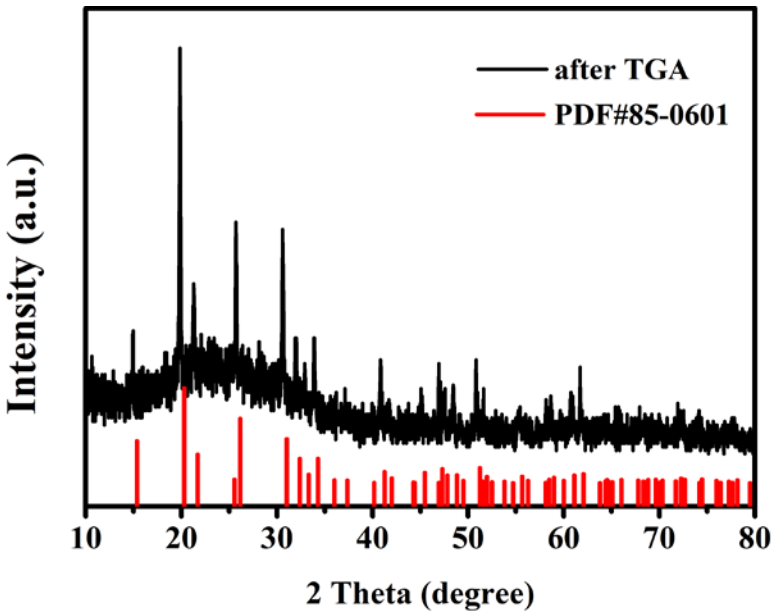

Fig. S7 XRD curves of VSe_2/rGO after TGA test.

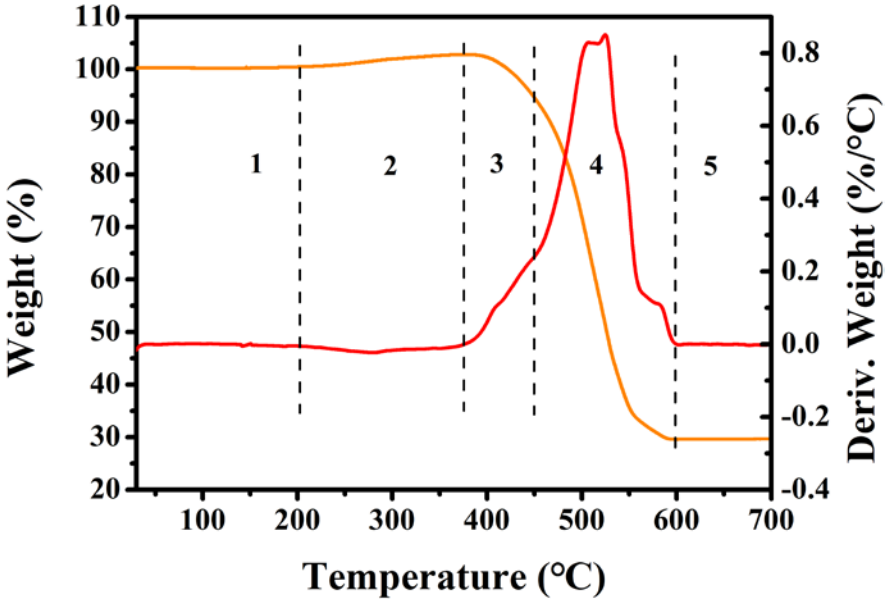

Fig. S8 Thermogravimetric analysis curves of VSe_2/rGO and it's thermogravimetric analysis differential curves.

As shown in Fig. 2h, from 200 °C to 380 °C, the weight of VSe_2 and the VSe_2/rGO not decrease as usually but rises a little with the increasing of heat-treated temperature. In order to under understand it well, the XRD of the

TGA test products were performed. As shown in Fig. S7, the diffraction peaks of the TGA products are well consist with the standard PDF card of V_2O_5. Combining with the relevant literature reports, a possible reaction process of VSe_2 during the heating process is proposed as follows:

1. 30 °C—200 °C: No phase change.
2. 200℃—380℃: VSe_2 reacts with O_2 to form V_2O_5 and SeO_2 ($4VSe_2+13O_2=2V_2O_5+2SeO_2$)
3. SeO_2 is volatilized at 300 ° C to 450 ° C.
4. rGO reacts with O_2 to form CO_2.
5. Residual V_2O_5.

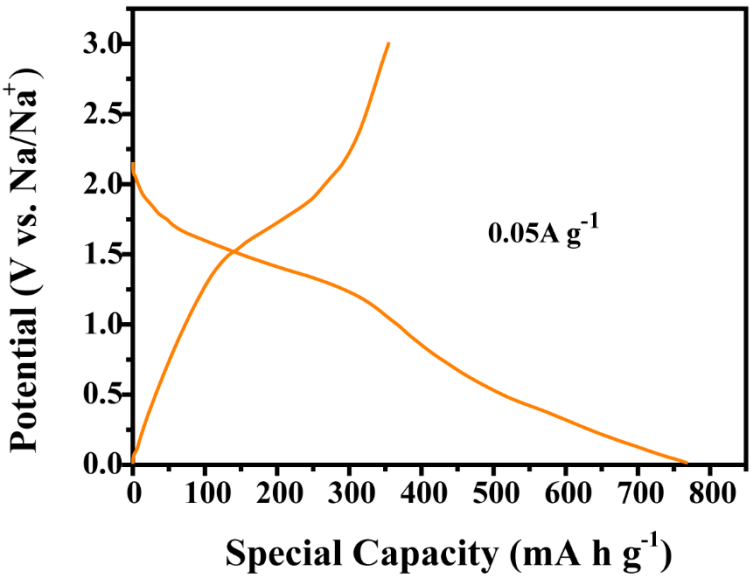

Fig. S9 Discharge/charge curves of VSe_2/rGO at 0.05 A g^{-1} for the first cycle.

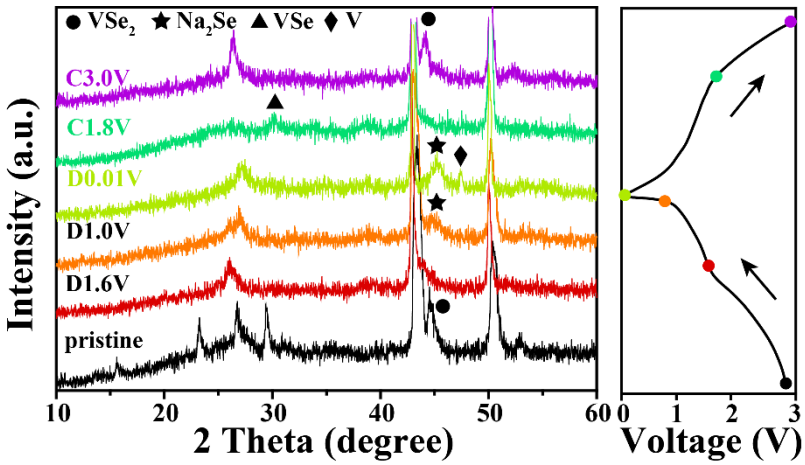

Fig. S10 Ex situ XRD patterns of VSe_2/rGO electrodes during charge/discharge.

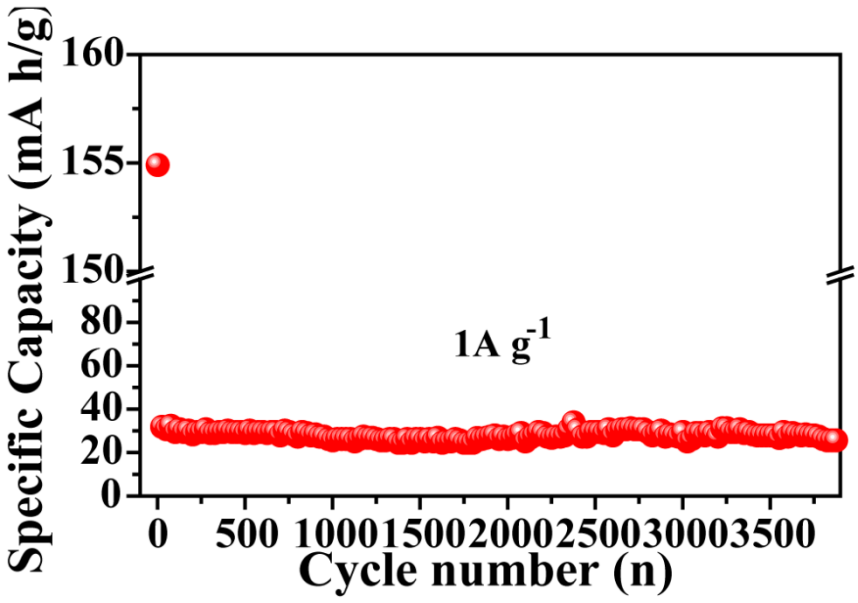

Fig. S11 Cycling stability of rGO aerogel 1A g^{-1}.

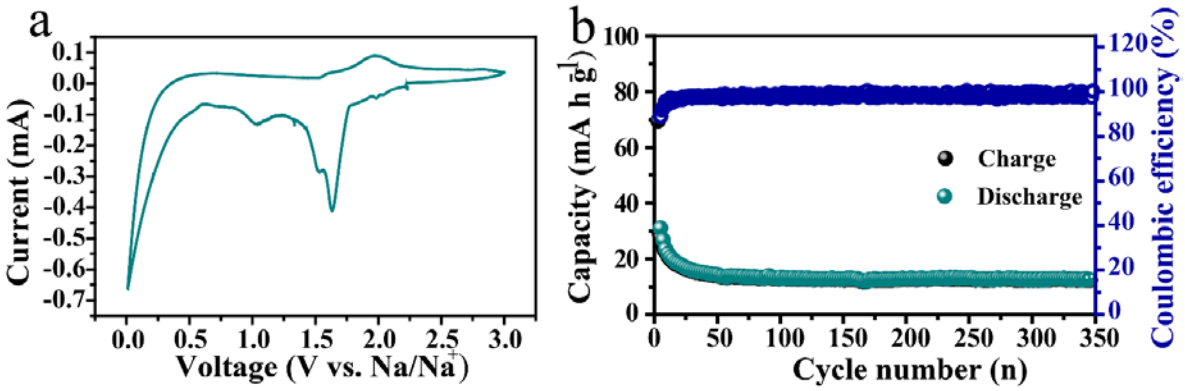

Fig. S12 (a) CV curves at a scan rate of 0.1 mV s^{-1} in 0.01–3.0 V of pure VSe_2. (b) Cycling stability of pure VSe_2.

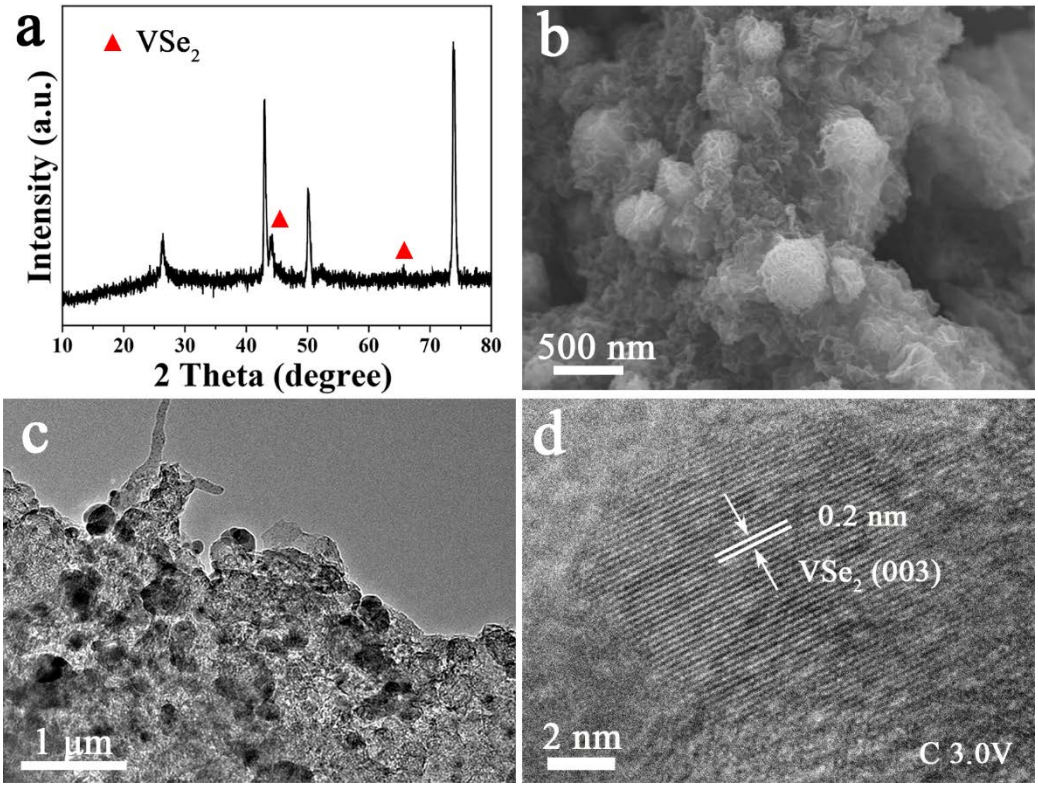

Fig. S13 (a) Ex-situ XRD curves. (b) FESEM images. (c) Low resolution TEM and HRTEM image of the active material after 1000 cycles.

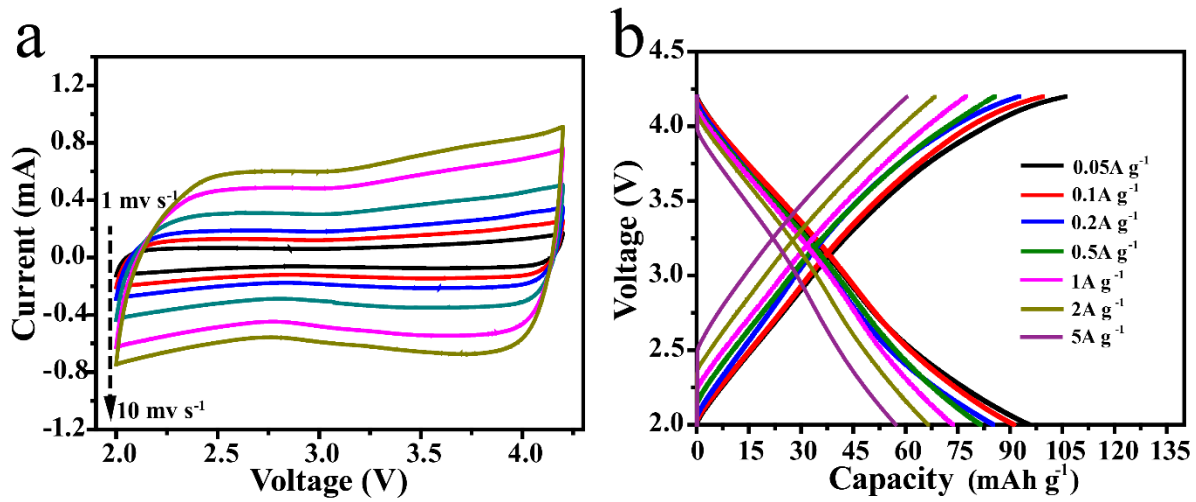

Fig. S14 (a) CV of AC from 1 to 10 mV s^{-1}. (b) Galvanostatic discharge/charge curves of AC from 0.05 A g^{-1} to 5 A g^{-1}.

The near-rectangular-shaped CV curves of AC (Fig. S14a) hardly changed as the sweep rate increases. As display in Fig. S14b, when the current density is 1A g^{-1}, the specific capacity of AC is about 75 mA h g^{-1}, which is about one-third of the VSe_2/rGO at the same current density. Therefore, we set the weight ratio of AC cathode to VSe_2/rGO anode about to 3:1.